

Characterization of mid-infrared single mode fibers as modal filters

A. Ksendzov,^{1,*} O. Lay,¹ S. Martin,¹ J. S. Sanghera,² L. E. Busse,² W. H. Kim,² P. C. Pureza,²
V. Q. Nguyen,² and I. D. Aggarwal²

¹Jet Propulsion Laboratory, California Institute of Technology 4800 Oak Grove Drive, Pasadena, California 91109, USA

²Naval Research Laboratory, Code 5606, 4555 Overlook Avenue, Washington, D.C. 20375, USA

*Corresponding author: alexander.ksendzov@jpl.nasa.gov

Received 27 July 2007; accepted 28 September 2007;
posted 10 October 2007 (Doc. ID 85674); published 9 November 2007

We present a technique for measuring the modal filtering ability of single mode fibers. The ideal modal filter rejects all input field components that have no overlap with the fundamental mode of the filter and does not attenuate the fundamental mode. We define the quality of a nonideal modal filter Q_f as the ratio of transmittance for the fundamental mode to the transmittance for an input field that has no overlap with the fundamental mode. We demonstrate the technique on a 20 cm long mid-infrared fiber that was produced by the U.S. Naval Research Laboratory. The filter quality Q_f for this fiber at 10.5 μm wavelength is 1000 ± 300 . The absorption and scattering losses in the fundamental mode are approximately 8 dB/m. The total transmittance for the fundamental mode, including Fresnel reflections, is 0.428 ± 0.002 . The application of interest is the search for extrasolar Earthlike planets using nulling interferometry. It requires high rejection ratios to suppress the light of a bright star, so that the faint planet becomes visible. The use of modal filters increases the rejection ratio (or, equivalently, relaxes requirements on the wavefront quality) by reducing the sensitivity to small wavefront errors. We show theoretically that, exclusive of coupling losses, the use of a modal filter leads to the improvement of the rejection ratio in a two-beam interferometer by a factor of Q_f . © 2007 Optical Society of America

OCIS codes: 060.2390, 060.2430, 060.2270.

1. Introduction

Modal filters are devices that propagate only a single spatial mode, such as single-mode waveguides or single mode fibers. By definition, the field at the ideal filter's output will have the shape of the fundamental (and only) mode of the filter [1–3]; all other components of the input field are removed. The quality of a nonideal modal filter is proportional to its ability to remove the input field components that have no overlap with the filter's fundamental mode (FM) and inversely proportional to the attenuation of the FM. Accordingly, we present a measurement technique for T_F , the transmittance for the FM, and T_A , the transmittance (leakage) for an antisymmetric input field that has no overlap with the filter's fundamental

mode. We define the quality of the filter as the ratio $Q_f = T_F/T_A$.

The application of interest is the observation of extrasolar planets. The observation using regular telescopes is impeded by the bright star, whose light overwhelms the faint image of a planet orbiting around it. The use of nulling interferometers for planet finding relies on suppressing the starlight by combining beams from two or more telescopes out of phase [4,5] as shown schematically in Fig. 1. The light received by the two telescopes passes through a delay line and an attenuator (needed for amplitude balancing). In principle, the starlight received by the two mirrors can be completely canceled if it is recombined at the detector exactly out of phase with the amplitudes exactly balanced (assuming an infinitely small star). The star and the planet are offset in angle on the sky so, at this delay line setting, the signal from the planet will not be canceled completely. Furthermore, by properly adjusting the interferometer

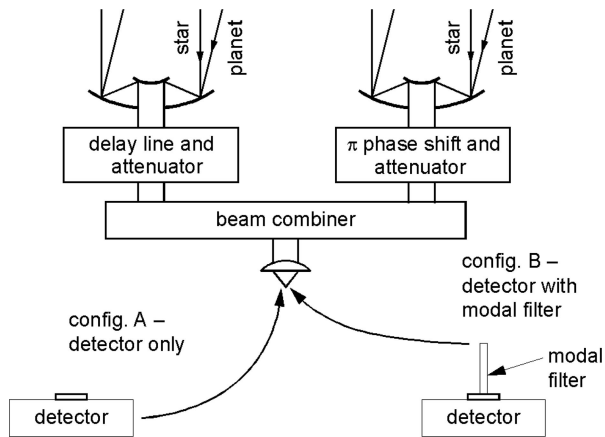


Fig. 1. Planet detection using a two-beam interferometer. Configurations with and without the use of a modal filter (denoted as A and B, respectively) are shown.

baseline, it is possible to maximize the planet's signal when the starlight is completely suppressed.

One of the impediments to this technique is the existence of wavefront errors in the telescopes due to mirror imperfections and misalignments—the difference between the wavefronts will cause residual star signal at the null. In particular, the requirements for wavefront ripple are so severe—approximately 2 nm rms at 10 μm wavelength (see Table 1 in [1]) that they most probably cannot be satisfied without wavefront conditioning. Such conditioning can be accomplished using modal filters. The insertion of an ideal modal filter in the beam path, as shown in Fig. 1, can equalize the shapes of the two fields incident on the detector—both fields will have the shape of the filter's FM—and, with proper relative phase and amplitude adjustment, bring about a perfect null [1]. A nonideal filter will improve the null depth to some degree; in Appendix A we calculate that, exclusive of coupling losses, the null depth improvement in a two-beam interferometer is equal to the filter's quality Q_f .

The presented technique is an improvement on measurements we reported previously [6]. First, it delivers independent measurement of T_F , which is important for designing the optical system and for optimizing the fiber fabrication. Unlike the well-known cut-back technique [7], this method is applicable to connectorized and sealed cables. In addition, the new method of measuring T_A does not rely on a deconvolution procedure, which is highly susceptible to noise and truncation in experimental results.

2. Measurement Technique: T_A

As mentioned in Section 1, the filtering action is based on the filter's ability to reject the input field that has no overlap with the filter's mode and, in an ideal device, should not reach the output. To assess the efficiency of this process, we created such an input field. To measure the transmittance T_A , we needed to determine the fraction of the input power that reaches the output in the device under test. Therefore we measured two quantities: the power incident on the filter, P_I ,

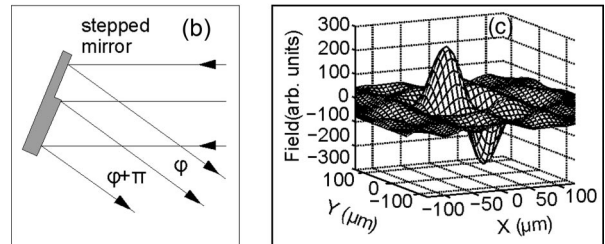
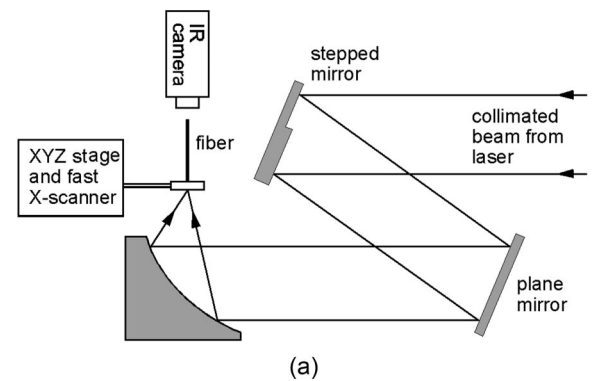


Fig. 2. (a) Experimental setup; (b) stepped mirror; (c) computed field distribution at the fiber's input.

and the power that leaked to the filter's output, P_L . We then found T_A from $T_A = P_L/P_I$.

The measurement setup is shown in Fig. 2(a). It is similar in concept to the fiber nulling setup of Haguener and Serabyn [8]. We used a quantum cascade laser operating at 10.5 μm wavelength with the coherence length much shorter than the length of the fiber. The input field was created by reflecting a collimated beam from a stepped mirror. As shown schematically in Fig. 2(b), the two halves of the mirror are offset such that the fields in the two halves of the reflected beam were shifted in phase by π .

The stepped mirror was fabricated as follows. We started with a regular 3 in. round mirror, and spun photoresist onto its front surface. The resist was then baked in an oven. Next, half of the surface was exposed to UV light and then developed in a standard photoresist developer, thereby forming a step. The surface was then coated with a layer of chromium (needed for adhesion) and gold using electron beam evaporation.

The calculated field distribution in the focal plane is shown in Fig. 2(c). The antisymmetric field has a node in the center and should not couple to the symmetric fundamental mode of the fiber when the center of the core is aligned with the center of the field distribution. To find the proper alignment, the fiber's input end was scanned in the focal plane using the XYZ stage, and the light intensity at the output was recorded as a function of the input end's position.

We found that scanning the XYZ stage was slow and therefore only convenient to find the approximate alignment. Once the approximate alignment was found, we used an electrostrictive fast scanner mounted on the stage to scan the beam in the X

direction—the direction in which the field is antisymmetric. This produced a large number of samples so that curve fitting could be used for finding the leakage signal P_L as described in Section 4.

To measure the power input into the filter, P_I , a pinhole sized to be greater than the fiber's mode field diameter was mounted in front of the fiber within Rayleigh distance from the fiber's end. Once the leakage signal was measured, the fiber was removed so that the power transmitted through the pinhole could be measured.

We used an infrared (IR) camera fitted with an IR lens to measure the input power transmitted through the pinhole and the output power from the fiber. The image of the source (the pinhole or the fiber) was intentionally blurred to avoid saturating the camera. This allowed us to cover the wide dynamic range between the weak signal at the minimum of the fiber transmittance and the strong signal measured from the pinhole. For every data point, the image acquired with the laser turned off was subtracted to eliminate background. We found that the reading was rather insensitive to the area of the IR sensor array we used—moving the image across the array we encountered $\sim 5\%$ variation. The camera output was recorded in “digital numbers” (DN)—arbitrary units proportional to the photon flux.

3. Measurement Technique: T_F

The transmittance for the fundamental mode T_F accounts for the Fresnel reflections from the two ends of the fiber and for the light absorption or scattering in the fiber. Again, unlike the well-known cut-back technique, the reported method is useful for characterizing losses in connectorized and sealed cable.

The fiber was illuminated by a CO_2 laser operating at $\sim 10.6 \mu\text{m}$ wavelength and the intensity of the transmitted light was recorded as the function of time. The optical path length was varied by slightly heating the fiber with a heat gun and then allowing it to cool. Since the coherence length of the CO_2 laser was much greater than the length of the fiber, the fiber behaved like a Fabry–Perot interferometer whose transmittance is sensitive to the heat-induced change of the fiber length and of the refractive index. This procedure resulted in intensity oscillations at the output (this technique will work in single mode fibers only—in multimode fibers the modal dispersion will wash out the oscillations). The amplitude of these oscillations is related to the reflectance of the fiber's ends and losses inside the fiber by the expression derived by Hakki and Paoli [9] for planar waveguides,

$$\alpha l = \ln R + \ln(I_+^{1/2} + I_-^{1/2}) - \ln(I_+^{1/2} - I_-^{1/2}), \quad (1)$$

where α is the absorption coefficient, l is the fiber's length, R is the reflectivity of the fiber's end which we determined from the refractive index of the core, and I_- and I_+ are the minimum and maximum values of the oscillating output, respectively. Equation (1) is used to determine the absorption coefficient α , which

accounts for losses inside the fiber due to absorption and scattering. To determine the total loss under operating conditions including reflections from the fiber's ends, this result for α was substituted into the well-known expression for the incoherent transmission through a slab of lossy material,

$$T_F = (1 - R)^2 e^{-\alpha l} / (1 - R^2 e^{-2\alpha l}). \quad (2)$$

Notice that this method only requires the knowledge of the reflectance R and of maxima and minima of the transmitted intensity; the knowledge of the temperature variations during the experiment and the fiber's thermal expansion coefficient is not required.

4. Results

We report results for a fiber cable produced by the U.S. Naval Research Laboratory (NRL) using chalcogenide glass [10]. The radiation escaping into the cladding was stripped out by coating the fiber with liquid gallium inside the cable. The design parameters of this fiber are presented in Table 1.

As can be seen, the fiber parameter V (sometimes referred to as normalized frequency [3]) at $10.5 \mu\text{m}$ is well below the critical value V_c of 2.405, above which the fiber becomes multimode. The fiber's far-field radiation pattern was measured using a detector mounted on a rotational stage with the fiber output at the center of the rotation circle. The pattern, shown in Fig. 3, has a smooth single-peak line shape. The Gaussian curve fit is also shown in Fig. 3; the near-Gaussian line shape is consistent with single mode behavior.

To characterize the coupling of the antisymmetric field into the fiber we scanned its input tip along the focal plane using an XYZ stage. The 3D graph of the output intensity distribution versus the fiber's tip position is shown in Fig. 4. The output intensity profile fulfills our expectations for single mode fibers: the peaks occur when the fundamental mode of the fiber is positioned at the maxima of the input field shown in Fig. 2(c), the minimum between the two peaks occurs when the node of the input field aligns with the center of the fundamental mode of the fiber. Ideally, at this point, the antisymmetric input field does not couple to the symmetric fundamental mode of the fiber, so the detected signal will be referred to as leakage.

Having found the position in the middle between the two peaks, we then used the fast scanner on the X stage to raster the beam in the X direction across the face of the fiber. The results of this one-dimensional scanning are shown in Fig. 5. The leakage signal P_L corresponds to the minimum between

Table 1. Design Parameters of the Fiber

Length (cm)	Core		Cladding		Normalized Frequency V
	Diameter (μm)	Refractive Index	Diameter (μm)	Refractive Index	
20	23	2.725	127	2.714	1.66

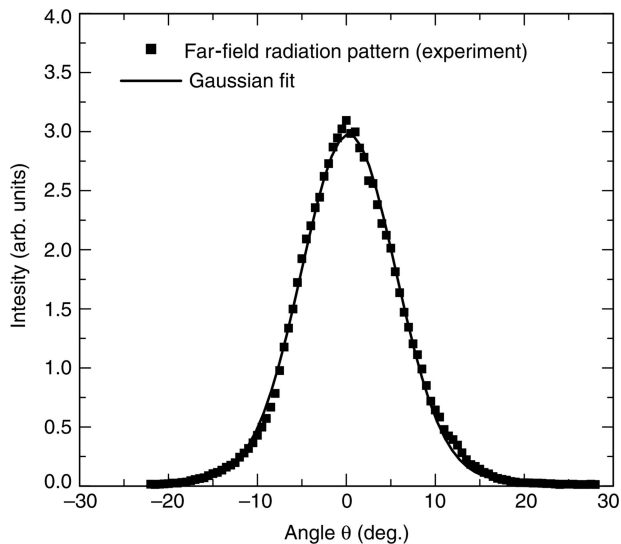


Fig. 3. Far-field radiation pattern of the NRL fiber. Gaussian fit is also shown.

the peaks. To improve accuracy, we obtained the minimum signal value by fitting the measurement result to a parabola near the minimum, as shown by the solid curve in Fig. 5. To evaluate the experimental uncertainty and further improve accuracy, we determined and averaged the minima of 88 consecutive measurements. This procedure resulted in P_L of (41 ± 12) DN.

To measure the power incident on the modal filter, P_I , after the scan was completed the fiber and the fiber bulkhead were removed with only the pinhole remaining in place. The power transmitted through the pinhole was measured using the same camera; the resulting power was $P_I = (1.05 \pm 0.05) \times 10^5$ DN. Thus we computed $T_A = P_L/P_I = (4 \pm 1) \times 10^{-4}$.

The results for the FM transmittance T_F were obtained as described in Section 3. The refractive index of the core at $10.6 \mu\text{m}$ wavelength was measured by spectroscopic ellipsometry using a polished plate

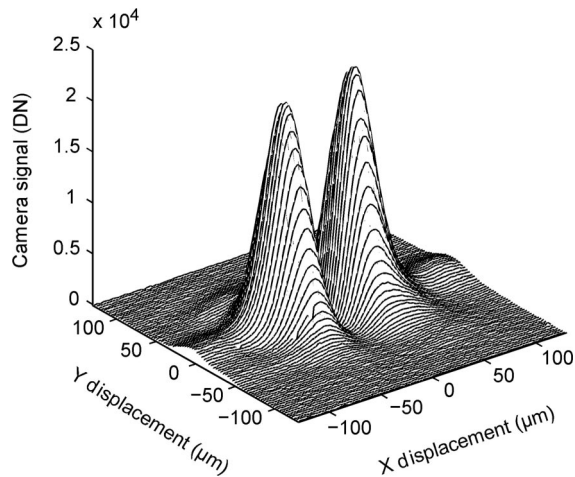


Fig. 4. Output intensity versus the NRL fiber position in the focal plane.

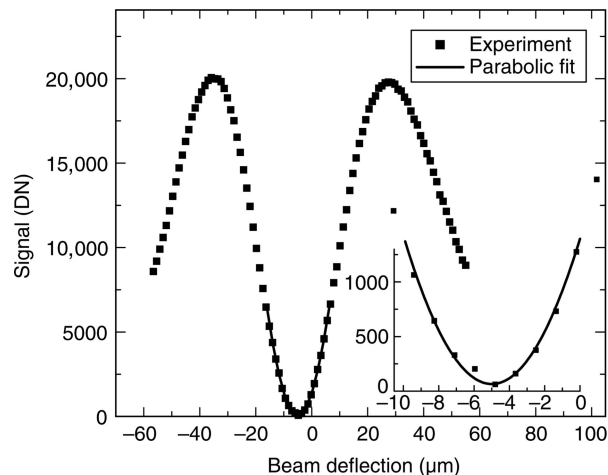


Fig. 5. Output intensity versus the NRL fiber position in the focal plane—one-dimensional scan. The solid curve shows parabolic fit near the minimum. Enlarged section of the plot near the minimum is shown in the inset. The minimum in this particular measurement is 65 DN. We averaged fit results of 88 such measurements to obtain the leakage power.

of the core material; the measured index is 2.725 ± 0.005 . Fresnel reflectance at the fiber's end R therefore is 0.2144 ± 0.002 . The time dependence of the transmitted signal during the fiber cooling is shown in Fig. 6(a). Five values of I_+ and I_- were determined by performing a parabolic fit to data near the successive maxima and minima [see Fig. 6(b)] and substituted into Eq. (1). Averaging of the results yielded αl of 0.367 ± 0.003 , which for the 20 cm long fiber corresponds to scattering and absorption losses of approximately 8 dB/m. Using Eq. (2), we obtained the transmittance for the FM, including Fresnel reflections, T_F , of 0.428 ± 0.02 . The resulting quality metric Q_f is 1000 ± 300 . In Appendix A we show that in a two-beam interferometer, exclusive of coupling

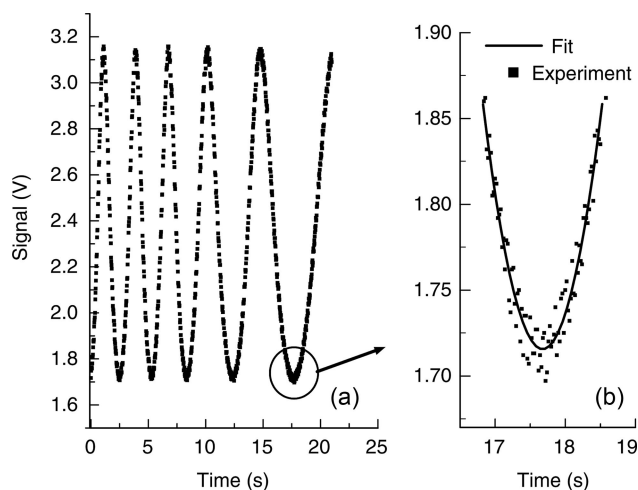


Fig. 6. Measurement of absorption in fiber using long coherence length laser. (a) Time dependence of the transmitted intensity during fiber cooling. (b) Parabolic data fit near the last minimum. Five values of I_+ and I_- were determined from such fits of successive maxima and minima.

losses, the use of a filter will improve the null depth by a factor of Q_f . The coupling losses depend on the coupling optics; the best power coupling efficiency that can be achieved without beam-shaping for a plane wave coupled into a step-index fiber at the single-mode cutoff is 0.78 [3].

5. Conclusions

We presented a technique for determining the modal filtering ability of single-mode fibers. Two parameters were measured: T_F , the transmittance for the fundamental mode, and T_A , the transmittance (leakage) for an input field that has no overlap with the fiber's mode. The quality of the filter was defined as the ratio $Q_f = T_F/T_A$. Our calculations show that, exclusive of coupling losses, the null depth improvement in a two-beam interferometer is given by Q_f . We have demonstrated the technique on an infrared fiber operating in the 10 μm spectral region. The total transmittance for the fundamental mode, including Fresnel reflections, is 0.428 ± 0.002 . The absorption and scattering losses in the fiber are approximately 8 dB/m. The filter quality Q_f for this fiber at the wavelength of 10.5 μm is 1000 ± 300 .

Appendix A

We calculate the relationship between the filter's quality Q_f and the improvement that can be achieved by inserting it in a two-beam interferometer. A commonly used figure of merit for nulling interferometers is the rejection ratio R , expressed as $R = P_C/P_D$, where P_D and P_C are the powers detected under the destructive and constructive interference conditions, respectively. Another commonly used quantity is the null depth, which is the inverse of R .

Consider a two-beam interferometer experiment, such as shown in Fig. 1. In configuration A the beams are recombined on the detector without the use of a modal filter. Let us denote the field and the power on the detector resulting from the illumination by the i th beam alone as $E_i(x, y)$ and P_i , respectively. The fields $E_1(x, y)$ and $E_2(x, y)$ are slightly different due to imperfect optical components and alignment errors. The overlap integral between the two fields, denoted as ξ , can be expressed as $\xi = \int_{A_x} e_1(x, y)e_2^*(x, y)dx dy$, where e_1 and e_2 are the fields E_1 and E_2 normalized: $\int_{A_x} e_1(x, y)e_1^*(x, y)dx dy = 1$. For two fields that are almost identical (i.e., $E_1(x, y) \approx E_2(x, y)$, exclusive of π phase shift), ξ is close to unity, so the parameter $\varepsilon = 1 - |\xi|$ is small. Under this assumption it can be shown that $P_C \approx 4P_1$, $P_D \approx 2\varepsilon P_1$, and the rejection ratio achieved without the wavefront conditioning, denoted as R_0 , can be expressed as

$$R_0 \approx (2/\varepsilon). \quad (\text{A1})$$

Now let us consider the system with an ideal modal filter inserted in front of the detector as suggested by Mennesson *et al.* [1] (Fig. 1, configuration B). By definition, the field at the ideal filter's output will have the shape of the fundamental (and only)

mode of the filter [1–3]. Therefore, the insertion of an ideal modal filter can equalize the shapes of the two fields incident on the detector, and with proper relative phase and amplitude adjustment, bring about a perfect null [1]. It can be shown that, if the difference between the wavefronts is caused by the random phase and amplitude ripple, the intensity of light incident on the filter's input is $P_{in} \approx 2\varepsilon P_1$ when the perfect null is achieved. At this point the field distribution at the filter's input has zero overlap with the filter's mode so, ideally, all this power is either radiated or dissipated [2,3].

A nonideal filter is different from the ideal one in two ways: (1) Only a fraction T_F of the fundamental mode power excited at the input reaches the detector. This factor accounts for the Fresnel reflections at both ends and for the absorption loss. Therefore, under the constructive interference conditions, the power reaching the detector is $P_C \approx 4T_F\eta P_1$, where η is the power efficiency of coupling of the light from the telescope into the fiber exclusive of Fresnel losses [2]. (2) Even though under the best nulling conditions the input field has no overlap with the filter's mode, a fraction T_A of the input power will leak to the detector, resulting in the detected power $P_D = T_A P_{in} \approx 2T_A\varepsilon P_1$. Therefore, the rejection ratio of the interferometer with an imperfect modal filter R_f can be expressed as

$$R_f \equiv P_C/P_D \approx (2/\varepsilon)(T_F\eta/T_A) = (T_F\eta/T_A)R_0. \quad (\text{A2})$$

Comparing Eqs. (A1) and (A2) we note that the improvement of the rejection ratio can be expressed as $(\eta T_F/T_A)$. The parameter η is the power coupling efficiency for the light focused into the filter exclusive of Fresnel losses. This parameter is characteristic of the interferometer's coupling optics but not of the filter itself. (When focusing a plane wave, the best match of the focusing optics to a step-index single mode fiber results in $\eta \approx 0.78$ at the single mode cutoff [3].) The leakage T_A is the fraction of the input power reaching the detector when the input field has no overlap with the filter's mode and T_F is transmittance for the filter's fundamental mode. The parameter $Q_f = T_F/T_A$ is the filter's characteristic; according to Eq. (A2) it constitutes the improvement of the rejection ratio exclusive of spatial coupling conditions.

This research was carried out at the Jet Propulsion Laboratory, California Institute of Technology, under a contract with the National Aeronautics and Space Administration.

References

1. B. Mennesson, M. Ollivier, and C. Ruilier, "Use of single-mode waveguides to correct the optical defects of a nulling interferometer," *J. Opt. Soc. Am. A* **19**, 596–602 (2002).
2. O. Wallner, W. R. Leeb, and P. J. Winzer, "Minimum length of a single-mode fiber spatial filter," *J. Opt. Soc. Am. A* **19**, 2445–2448 (2002).
3. A. W. Snyder and J. D. Love, *Optical Waveguide Theory* (Chapman and Hall, 1983).

4. R. N. Bracewell and R. H. MacPhie, "Searching for nonsolar planets," *Icarus* **38**, 136–147 (1979).
5. K. Wallace, G. Hardy, and E. Serabyn, "Deep and stable interferometric nulling of broadband light with implications for observing planets around nearby stars," *Nature* **406**, 700–702 (2000).
6. A. Ksendzov, E. Bloemhof, V. White, J. K. Wallace, R. O. Gappinger, J. S. Sanghera, L. E. Busse, W. J. Kim, P. C. Pureza, V. Q. Nguyen, L. D. Aggarwal, S. Shalem, and A. Katzir, "Measurement of spatial filtering capabilities of single mode infrared fibers," *Proc. SPIE* **6268**, 626838 (2006).
7. R. G. Brown and B. N. Derick, "Plastic fiber optics. II: Loss measurements and loss mechanisms," *Appl. Opt.* **7**, 1565–1569 (1968).
8. P. Haguenaer and E. Serabyn, "Deep nulling of laser light with a single-mode-fiber beam combiner," *Appl. Opt.* **45**, 2749–2754 (2006).
9. B. W. Hakki and T. L. Paoli, "Gain spectra in GaAs double-heterostructure injection lasers," *J. Appl. Phys.* **46**, 1299–1306 (1975).
10. I. D. Aggarwal and J. S. Sanghera, "Development and applications of chalcogenide glass optical fibers at NRL," *J. Optoelectron. Adv. Mater.* **4**, 665–678 (2002).